Novel receiving coil structure for improving efficiency and power transfer capability of resonant inductive coupling wireless power transfer

T. Honjo*, T. Koyama*, K. Umetani*, and E. Hiraki*

* Okayama University,
3-1-1 Tshushimanaka, Kita-ku,
Okayama, Japan.

Published in: 2016 19th International Conference on Electrical Machines and Systems (ICEMS)

https://ieeexplore.ieee.org/document/7837238

Novel Receiving Coil Structure for Improving Efficiency and Power Transfer Capability of Resonant Inductive Coupling Wireless Power Transfer

T. Honjo*, T. Koyama*, K. Umetani*, and E. Hiraki*
* Okayama University, 3-1-1 Tshushimanaka, Kita-ku, Okayama, Japan.

***Abstract*—Resonant inductive coupling wireless power transfer (RIC-WPT) is attractive as a convenient power supply method to small mobile apparatus. However, limited size of the receiving coil can limit the efficiency and the power transfer capability. This paper addresses this difficulty by proposing a novel receiving coil structure. The proposed structure has a coil wound on a drum core with a thin axis. The top and the bottom of the drum core has large surface area to effectively collect the magnetic flux for large mutual inductance. In addition, the thin axis can reduce the wire length, thus reducing the parasitic AC resistance. The AC resistance is further reduced by suppressing the proximity effect. Simulation supported probable improvement in the efficiency as well as the power transfer capability. In addition, experiment verified that the proposed structure improved the efficiency by 66% and the power transfer capability by 109%.**

***Index Terms*—Eddy current, Inductive coupling, Magnetic structure, Wireless power transfer.**

I. Introduction

Resonant inductive coupling wireless power transfer [1]–[12] (RIC-WPT) is attracting growing attention as a convenient power supply method to small mobile apparatus, such as mobile phones and capsule endoscopy [2][4][13]. A typical RIC-WPT system consists of a transmitting resonator and a receiving resonator, as shown in Fig. 1. The coils of these resonators are magnetically coupled each other. Resonance frequencies of these resonators are designed to be close each other so that the resonance in the transmitting coil can induce the resonance also in the receiving resonator.

In the RIC-WPT system, small voltage applied to the transmitting resonator can induce large resonance current in the transmitting coil. Furthermore, small voltage induction in the receiving coil can excite large resonance in the receiving coil. Therefore, RIC-WPT is effective even under weak magnetic coupling, as is often the cases for small-sized receiving coils of small mobile apparatus.

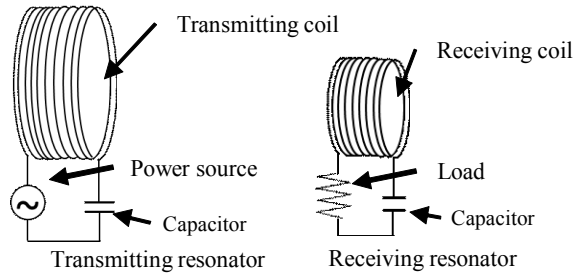

Fig.1. Resonant inductive coupling wireless power transfer system.

In spite of this attractive feature of RIC-WPT, limited size of the receiving coil still tends to restrict the efficiency as well as the power transfer capability. Therefore, improvement in the efficiency and the power transfer capability is intensely required for practical applications of RIC-WPT to small mobile apparatus.

As widely known [4][14], the maximum efficiency of RIC-WPT systems can be determined by the figure-of-merit F, defined as

$$F = k^2 Q_{\mathrm{T}} Q_{\mathrm{R}} = \frac{Q_{\mathrm{T}} M^2}{r_{\mathrm{R}} L_{\mathrm{T}} \sqrt{L_{\mathrm{R}} C_{\mathrm{R}}}}, \tag{1}$$

where k is the magnetic coupling coefficient; M is the mutual inductance; Q_{T} and L_{T} are the Q factor and inductance of the transmitting resonator; Q_{R}, L_{R}, C_{R}, and r_{R} are the Q factor, inductance, series-connected capacitance, and parasitic AC resistance of the receiving resonator.

This equation indicates that the receiving coil is required to increase M^2/r_{R} for better efficiency because $L_{\mathrm{R}}C_{\mathrm{R}}$ is commonly determined by the specification on the resonant frequency.

Similar result is also obtained for the power transfer capability. As shown in the appendix, M^2/r_{R} is also an essential factor that characterizes the maximum power transfer of RIC-WPT systems. Hence, higher M^2/r_{R} can improve the efficiency as well as the power transfer capability.

An effective strategy for higher M^2/r_{R} is to increase M. For this purpose, two approaches are widely utilized for the receiving coil design: One is to wind the receiving coils to cover large area; and the other is to wind the receiving coil on a magnetic core, as exemplified in [15]. However, the former increases r_{R} because this requires long wire length. Furthermore, the latter also increases r_{R} in many cases due to the proximity effect because the magnetic core often generates intense local magnetic field near the wire, causing large eddy current in the wire.

Therefore, these approaches may hinder effective improvement in M^2/r_R due to increased r_R.

The purpose of this paper is to address this difficulty by proposing a magnetic structure that can effectively improve the factor M^2/r_R. This magnetic structure can reduce r_R; furthermore, it can implement similar value for M as the aforementioned approaches.

The following discussion consists of four sections. Section II presents the proposed magnetic structure. Sections III and IV present the simulation and the experiment, respectively, to verify improvement in the factor M^2/r_R compared with the aforementioned approaches. Finally, section V gives conclusions.

II. Proposed Magnetic Structure

This section presents the proposed magnetic structure in comparison with the conventional magnetic structure. In this paper, the conventional structure is assumed to utilize the two aforementioned approaches for improving the mutual inductance M.

Figure 2 depicts the proposed and conventional receiving coil structures. The conventional structure has a coil on a cylinder core. The magnetic core was designed to have as large cross-sectional area as possible, in order to maximize the area covered by the receiving coil. On the other hand, the proposed structure has a coil on a drum core with a thin axis. The top and the bottom of the core are designed to cover as large area as possible, whereas the axis is designed to have extremely small cross-sectional area compared with the top and bottom of the core. As a result, the proposed structure can be designed to occupy the same volumetric area as the conventional structure.

The top of the core has the same diameter in both structures. Hence, both of the structures can collect almost the same flux from the transmitting coil. Therefore, the proposed structure can have similar value for M as the conventional structure.

As for the parasitic AC resistance r_R, the proposed structure can reduce r_R, compared with the conventional structure, because

1. Total wire length is smaller owing to the thin axis;
2. Intense magnetic field is avoided near the wire to prevent the proximity effect from causing the large eddy current in the wire.

The former reason is apparent. Therefore, the second reason is discussed below.

According to the electromagnetism of the linear media, the magnetic flux lines turning around a corner tend to concentrate near the corner, causing inhomogeneity of the magnetic flux density [16][17]. As a result, the flux density tends to be large near the edge of the winding because the flux lines turn there at comparatively large curvature. As for the conventional structure, the flux lines turn mainly in the air near the winding edge. Therefore, large flux density at the winding edge results in intense magnetic field because of low permeability of the air, thus inducing large eddy current inside the wire near the winding edge. Therefore, the conventional structure tends to suffer from large parasitic AC resistance.

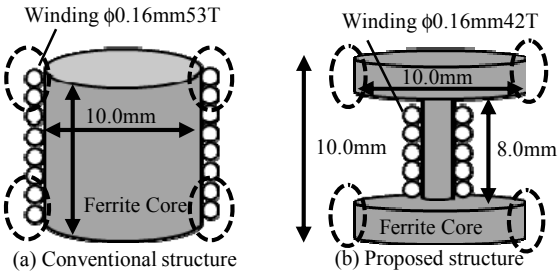

(a) Conventional structure (b) Proposed structure

Fig. 2. Conventional and proposed receiving coil structures.

TABLE I
Specifications of the Simulation Models

	Transmitting coil	Conventional structure	Proposed structure
Coil diameter	Inner:470mm Outer:590mm	10mm	2mm
Wire diameter	3.0mm	0.16mm	0.16mm
Number of turns	10 Turns	53 Turns	42 Turns
Core dimension	-	10mm	10mm
Self-inductance	72μH	82μH	67μH

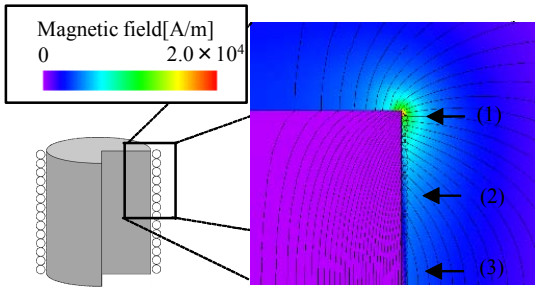

(a)Conventional structure

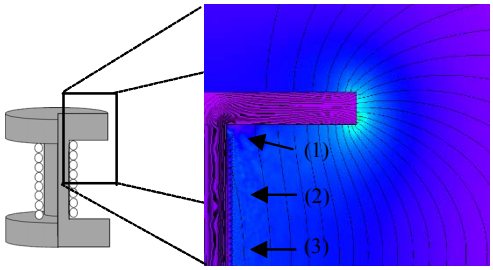

(b)Proposed structure

Fig. 3. Simulation results of the magnetic field. Solid lines are the flux lines.

On the other hand, the flux lines turn mainly in the magnetic core in the proposed structure because the winding edge is covered with the magnetic core. In this case, the large flux density does not lead to intense magnetic field owing to large permeability of the core, thus suppressing induction of the eddy current in the wire. Therefore, the proposed structure can reduce r_R in comparison with the conventional structure.

Consequently, the proposed structure can be expected to improve the factor M^2/r_R, leading to larger power transfer capability as well as higher efficiency.

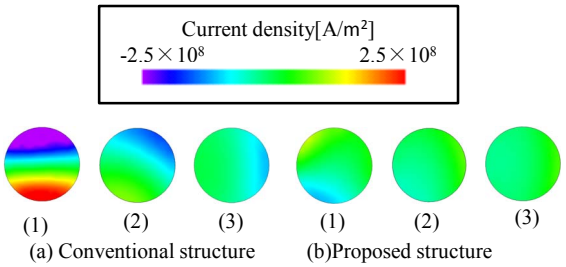

Fig. 4. Current distribution in the wire at points (1)–(3) in Fig. 3.

TABLE II
SIMULATION RESULTS OF THE FACTOR M^2/r_R

	Conventional structure	Proposed structure
AC resistance	7.0Ω	0.38Ω
Mutual inductance	97nH	72nH
M^2/r_R	$1.3\times10^{-15}H^2/\Omega$	$1.4\times10^{-14}H^2/\Omega$

III. SIMULATION

Simulation was carried out to verify the basic principles of the proposed structure as well as improvement in M^2/r_R, in comparison with the conventional structure. Specifications of the simulation models were presented in Table I. Simulation models have the same geometry as in Fig. 2. The receiving coils of these models were made of the same wire of ϕ0.16mm. The lossless ferrite core with the same B-H curve as Hitachi Metals ML12D was employed as the magnetic core material. Therefore, the AC resistance r_R was contributed only by the copper loss. Simulator was JSOL Corp. JMAG 14.0.

Figure 3 shows the simulation results of the magnetic field when the receiving coil current is 1.0Apeak, 800kHz. As can be seen in the figure, intense magnetic field appears near the edge of the winding in the conventional structure. On the other hand, the intense magnetic field is suppressed near the winding in the proposed structure, as can be expected from the previous section. The curves in the flux lines corresponded to the points of the intense magnetic field in Fig. 3, which is consistent with the theory.

Figure 4 shows the current distribution in the wire at three points presented in Fig. 3. As for the conventional structures, the large eddy current was induced in the wire near the edge of the winding, where intense magnetic field appeared in Fig. 3. On the other hand, the current flows homogeneously in the wire of the proposed structure even near the edge of the winding. This is also consistent with the theory.

Finally, the mutual inductance M and the AC resistance r_R were evaluated. Table II shows the result. The proposed structure was found to have similar value for M as the conventional structure, although M was slightly reduced by 24%. As for the AC resistance, great reduction was found in the proposed structure. The results indicate that the proposed structure reduced r_R into 5.4% of that of the conventional structure. As a result, the proposed structure increased the factor M^2/r_R by 11 times approximately, suggesting effectiveness of the proposed structure for improving the efficiency and the power transfer capability.

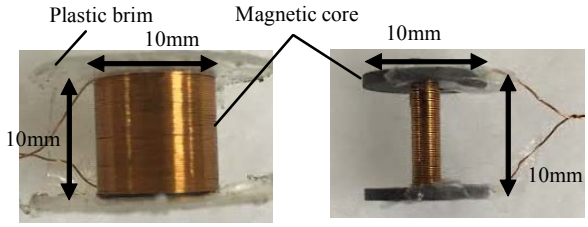

Fig. 5. Experimental receiving coil.

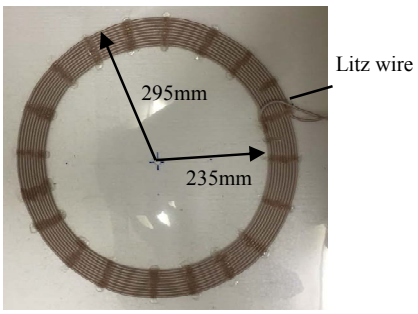

Fig. 6. Experimental transmitting coil.

TABLE III
SPECIFICATIONS OF THE EXPERIMENTAL RESONATORS

	Transmitting Coil	Conventional Structure	Proposed Structure
Coil diameter	Inner: 470mm, Outer: 590mm.	10mm	2mm
Number of turns	10 turns	53 turns	42 turns
Self-inductance	52μH	73μH	67μH
Capacitance	761pF	545pF	583pF
Load resistance	—	8.5Ω† 9.0Ω‡	1.3Ω† 1.5Ω‡

The receiving coil is placed at the distance of 300mm from the transmitting coil.
† The load resistance in the experiment of the efficiency
‡ The load resistance in the experiment of the power transfer capability.

TABLE IV
EXPERIMENTAL RESULTS OF THE FACTOR M^2/r_R

	Conventional structure	Proposed structure
AC resistance	8.5Ω	1.3Ω
Mutual inductance	44nH	28nH
M^2/r_R	$2.2\times10^{-16}H^2/\Omega$	$6.1\times10^{-16}H^2/\Omega$

IV. EXPERIMENT

In addition to the simulation, an experiment was carried out to verify improvement in the efficiency and the power transfer capability by the proposed structure. Figure 5 presents the photographs of the experimental receiving coils of the proposed and conventional structures. Specifications of the experimental transmitting and receiving resonators are presented in Table III. The

same wire of ϕ0.16mm was employed for the receiving coils. The core material employed for the receiving coil structures was FDK Corp. 7H20 [18]. In this experiment, we employed a transmitting resonator presented in Fig. 6. Specifications of the transmitting resonator are also presented in Table III.

A. AC Resistance and Mutual Inductance

First, we evaluated the AC resistance r_R and the mutual inductance M. The AC resistance of the receiving coil was obtained by measuring the Q factor of the receiving resonator when the load resistance was set at zero. The mutual inductance was measured between the transmitting coil and the receiving coil, when the receiving coil is placed with the distance of 300mm from the transmitting coil. In the measurement of the mutual inductance, we applied the sinusoidal current of 800kHz, 1.0Arms to the transmitting coil. Then, the voltage induction of the receiving coil is measured to obtain the mutual inductance.

Table IV presents the results. Although the proposed structure showed reduction in M by 46% compared with the conventional structure, great reduction of r_R contributed to improvement in M^2/r_R. The factor M^2/r_R of the proposed structure was 2.8 times as large as that of the conventional structure.

However, the AC resistance r_R measured in the proposed structure was approximately three times as large as that predicted by the simulation, although r_R of the conventional structure showed comparatively better agreement with the simulation. The reason can be explained by the iron loss, which was not considered in the simulation.

Because the proposed structure has a far thinner axis than the conventional structure, large magnetic flux density is induced in the axis by the self-inductance, thus increasing the AC resistance. Note that the top and the bottom of the proposed structure offers larger cross-sectional area for the magnetic flux than the axis. Therefore, the iron loss of the top and the bottom is expected to be small. As a result, we can roughly estimate the AC resistance contributed by the iron loss by calculating the iron loss in the axis.

We denote the effective value of the total AC flux and the AC flux density of the axis induced by the self-inductance L_R as ϕ and B, respectively. Then, ϕ and B can be obtained as

$$N_R\phi = L_R i, \quad B = \frac{\phi}{S} = \frac{L_R i}{SN_R}, \tag{2}$$

where i is the effective current of the receiving coil, N_R is the number of turns of the receiving coil, and S is the cross-sectional area of the axis.

According to Steinmetz equation, the iron loss per unit volume is approximately proportional to the square of the effective value of the magnetic flux density. If we denote the proportionality coefficient as k_S, the total iron loss P_{iron} of the axis and the AC resistance r_{iron} contributed by the iron loss can be estimated as

$$P_{iron} = k_S B^2 S\ell = \frac{k_S L_R^2 \ell}{SN_R^2} i^2, \quad \therefore r_{iron} = \frac{k_S L_R^2 \ell}{SN_R^2}, \tag{3}$$

where ℓ is the height of the core.

The value r_{iron} was estimated as 0.8Ω in the proposed structure and 0.02Ω in the conventional structure approximately. (The coefficient k_S is estimated based on the datasheet [18].) Therefore, r_{iron} can explain most of the difference between the simulation and the experiment of the proposed structure.

As we can see above, the proposed structure can improve M^2/r_R by reducing the copper loss. However, the excessively thin axis can cause significant iron loss. Therefore, optimization of the diameter of the axis may further reduce the parasitic AC resistance to maximize M^2/r_R.

B. Efficiency

Next, we evaluated the efficiency. In this experiment, the current of the transmitting coil was set at 1.0Arms, 800kHz. Then, the efficiency was calculated based on the measurement of the input power and the load power. The load resistance was set so that the experimental systems can achieve the maximum efficiency. The load resistance was calculated based on the theory presented in [5]. As a result, the load resistance was set at 1.3Ω for the proposed structure and 8.5Ω for the conventional

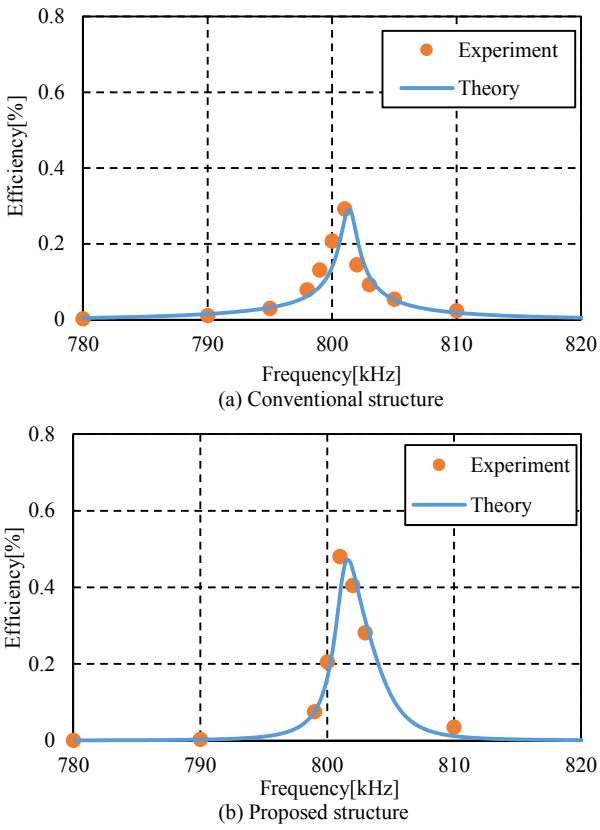

Fig. 7. Experimental results of the efficiency.

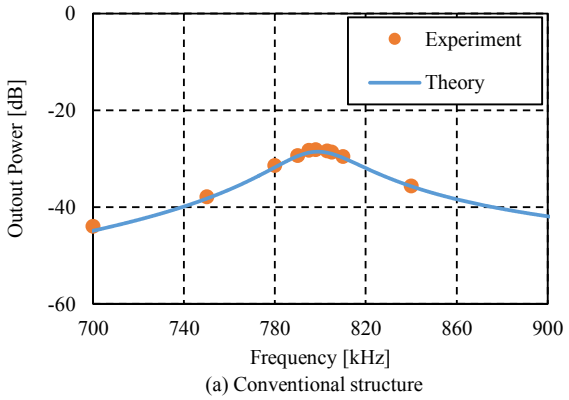

(a) Conventional structure

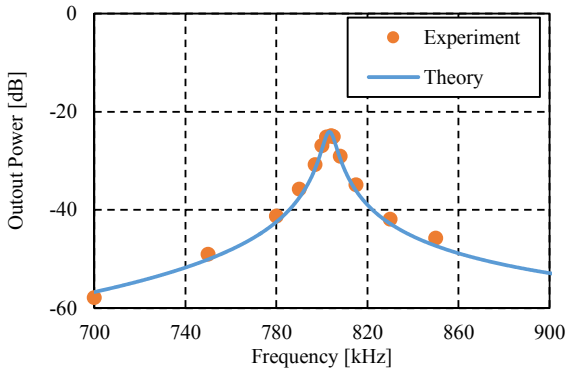

(b) Proposed structure

Fig. 8. Experimental results of the maximum output power.

structure, respectively.

Figure 7 shows the result. The solid line is the theoretical line calculated based on [5] using the parameters presented in Table III and Table IV. The result revealed that the maximum efficiency was improved by 66% in the proposed structure in comparison with the conventional structure, as is expected from the theory.

C. Power Transfer Capability

Finally, we evaluated the power transfer capability. In this experiment, the current of the transmitting coil was set at 1.0Arms, 800kHz. The load resistance was set so that the systems can output the maximum power to the load. The load resistance was calculated based on (10). As a result, the load resistance was set at 1.5Ω for the proposed structure and 9.0Ω for the conventional structure, respectively.

Then, we measured the dependency of the output power on the frequency. Figure 8 shows the result. The solid line is the theoretical line calculated based on (10) using the parameters presented in Table III and Table IV. The result also revealed effectiveness of the proposed structure because the maximum output power was improved by 109% in the proposed structure compared with the conventional structure, as is expected from the theory.

V. Conclusions

Wireless power transfer to small mobile apparatus often suffers from low efficiency and low power transfer capability due to limited size of the receiving coil. This difficulty is addressed in this paper by proposing an effective magnetic structure for the receiving coils of RIC-WPT. The proposed structure can improve the ratio of square of the mutual inductance to the parasitic AC resistance, which is the factor that determines the efficiency as well as the power transfer capability. Simulation supported the basic principles of the proposed structure as well as improvement in this factor. In addition, experiment verified improvement in the efficiency and the power transfer capability, supporting effectiveness of the proposed structure for practical applications of RIC-WPT to small mobile apparatus.

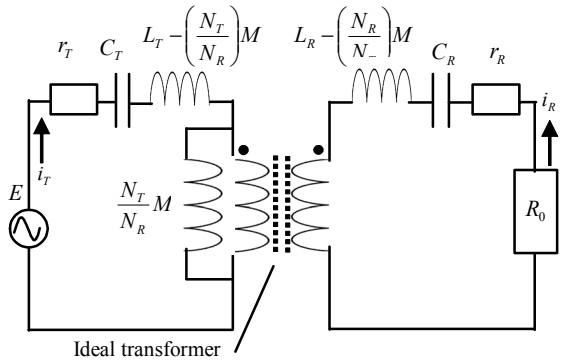

Fig. 9 Equivalent circuit model of the RIC-WPT system.

Appendix

This appendix analyzes a RIC-WPT system to show that the maximum output power is dependent on the factor M^2/r_R, similarly as the efficiency. In addition, this appendix derives the optimum load resistance that gives the maximum output power. The following discussion is based on the equivalent circuit model of the RIC-WPT system shown in Fig. 9. Symbols E, r_T, C_T, N_T, R_o, i_T, and i_R are the effective value of the voltage of the power supply, the parasitic AC resistance of the transmitting coil, the series-connected capacitance of the transmitting resonator, the number of turns of the transmitting coil, the load resistance, the effective value of the transmitting coil current, and the effective value of the receiving coil current, respectively.

According to Fig. 9, we obtain

$$E = i_T\left[r_T + j\left\{\omega L_T - \left(\frac{N_T}{N_R}\right)\omega M - \frac{1}{\omega C_T}\right\}\right] + \left\{i_T + \left(\frac{N_R}{N_T}\right)i_R\right\}\left(\frac{N_T}{N_R}\right)j\omega M, \tag{4}$$

$$0 = i_R\left[r_R + R_o + j\left\{\omega L_R - \left(\frac{N_R}{N_T}\right)\omega M - \frac{1}{\omega C_R}\right\}\right] + \left\{\left(\frac{N_T}{N_R}\right)i_T + i_R\right\}\left(\frac{N_R}{N_T}\right)j\omega M, \tag{5}$$

where ω is the angular frequency. Eliminating i_T from (4) and (5), we can obtain the output power P_{out} as

$$P_{out} = R_o \left| i_R \right|^2 = \frac{\omega^2 M^2 E^2 R_o}{\left| \alpha \right|^2}. \quad (6)$$

where α is defined as

$$\alpha = \left\{ r_T + j(\omega L_T - \frac{1}{\omega C_T}) \right\} \left\{ R_o + r_R + j(\omega L_R - \frac{1}{\omega C_R}) \right\} + \omega^2 M^2. \quad (7)$$

Now, we assume that the system is in the resonance. For convenience, we assume that the frequency dependency of the output power has only one peak because the magnetic coupling is commonly small in wireless power transfer. Hence, we impose

$$\omega = \frac{1}{\sqrt{L_T C_T}} = \frac{1}{\sqrt{L_R C_R}}. \quad (8)$$

Then, P_{out} can be expressed as

$$P_{out} = \frac{\omega^2 M^2 E^2}{\left(r_T \sqrt{R_o} + \frac{r_T r_R + \omega^2 M^2}{\sqrt{R_o}} \right)^2}. \quad (9)$$

Therefore, P_{out} takes the maximum value P_{out_max} at the optimum load resistance R_{o_opt}. These values are determined from (9) as

$$P_{out\_max} = \frac{\omega^2 E^2}{4 r_T \left(\omega^2 + \frac{r_T r_R}{M^2} \right)}, \quad R_{o\_opt} = \frac{r_T r_R + \omega^2 M^2}{r_T}. \quad (10)$$

The result indicates that the factor M^2/r_R determines the maximum output power and that larger factor can improve P_{out_max}.

REFERENCES

[1] Z. N. Low, R. A. Chinga, R. Tseng, "Design and test of a high-power high-efficiency loosely coupled planar wireless power transfer system," *IEEE Trans. Ind. Electron.*, vol. 56, no. 5, pp1801–1812, May 2009.

[2] B. L. Cannon, J. F. Hoburg, D. D. Stancil, and S. C. Goldstein, "Magnetic resonant coupling as a potential means for wireless power transfer to multiple small receivers," *IEEE Trans. Power Electron.*, vol. 24, no. 7, pp. 1819–1825, Jul. 2009.

[3] T. Imura and Y. Hori, "Maximizing air gap and efficiency of magnetic resonant coupling for wireless power transfer using equivalent circuit and Neumann formula," *IEEE Trans. Ind. Electron.*, vol. 58, no. 10, pp. 4746–4752, Oct. 2011.

[4] A. K. RamRakhyani and G. Lazzi, "On the design of efficient muti-coil telemetry system for biomedical implants," *IEEE Trans. Biomed. Circuit Syst.*, vol. 7, no. 1, pp. 11–23, Feb. 2013.

[5] I. Awai, "Basic characteristics of "Magnetic resonance" wireless power transfer system excited by a 0 ohm power source," *IEICE Electron. Express*, vol. 10, no. 21, pp. 1–13, Nov. 2013.

[6] R. Huang, B. Zhang, D. Qiu, and Y. Zhang, "Frequency splitting phenomena of magnetic resonant coupling wireless power transfer," *IEEE Trans. Magn.*, vol. 50, no. 11, 8600204, Nov. 2014.

[7] D. Ahn and S. Hong, "Wireless power transfer resonance coupling amplification by load-modulation switching controller," *IEEE Trans. Ind. Electron.*, vol. 62, no. 2, pp. 898–909, Feb. 2015.

[8] V. Jiwariyavej, T. Imura, and Y. Hori, "Coupling coefficients estimation of wireless power transfer system via magnetic resonance coupling using information from either side of the system," *IEEE J. Emerg. Sel. Topics Power Electron.*, vol. 3, no. 1, pp. 191–200, Mar. 2015.

[9] H. Li, J. Li, K. Wang, W. Chen, and X. Yang, "A maximum efficiency point tracking control scheme for wireless power transfer systems using magnetic resonant coupling," *IEEE Trans. Power Electron.*, vol. 30, no. 7, pp. 3998–4008, Jul. 2015.

[10] G. Buja, M. Bertoluzzo, and K. N. Mude, "Design and experimentation of WPT charger for electric city car," *IEEE Trans. Ind. Electron.*, vol. 62, no. 12, pp. 7436–7447, Dec. 2015.

[11] M. R. V. Moghadam and R. Zhang, "Multiuser wireless power transfer via magnetic resonant coupling: performance analysis, charging control, and power region characterization," *IEEE Trans. Signal Inform. Process. Over Networks*, vol. 2, no. 1, pp. 72–82, Mar. 2016.

[12] H. Kim, C. Song, D.-H. Kim, D. H. Jung, I.-M. Kim, Y.-I. Kim, J. Kim, S. Ahn, and J. Kim, "Coil design and measurements of automotive magnetic resonant wireless charging systems for high-efficiency and low magnetic field leakage," *IEEE Trans. Mirow. Theory Techn.*, vol. 64, no. 2, pp. 383–400, Feb. 2016.

[13] G. Ciuti, A. Menciassi, P. Dario, "Capsule endoscopy: from current achievements to open challenges," *IEEE Rev. Biomed. Eng.*, vol. 4, pp. 59–72, Oct. 2011.

[14] M. Pinuela, D. C. Yates, S. Lucyszyn, and P. D. Mitcheson, "Maximising DC to load efficiency for inductive power transfer," *IEEE Trans. Power Electron.*, vol. 28, no. 5, pp. 2437–2447, Aug. 2012.

[15] R. Itoh, Y. Sawahara, T. Ishizaki, and I. Awai, "Construction of a secure wireless power transfer system for robot fish," in *Proc. IEEE Wireless Power Transfer Conf.*, F3.6, pp. 1–4, May 2015.

[16] K. Umetani, "Improvement of saturation property of iron powder core by flux homogenizing structure," IEEJ Trans. Elect. Electron. Eng., vol. 8, no. 6, pp. 640-648, Sep. 2013.

[17] K. Umetani, Y. Itoh, and M. Yamamoto, "A detection method of DC magnetization utilizing local inhomogeneity of flux distribution in power transformer core," in *Proc. IEEE Energy Conversion Congr. Expo.*, Pittsburgh, PA, 2014, pp. 3739-3746.

[18] FDK Corp., Datasheet of 7H series material. [Online]. Available: http://www.fdk.co.jp/cyber-j/pdf/fe_7h.pdf. Accessed Jul. 28, 2016. (in Japanese)